Journal of Applied Physics

Theoretical efficiency limit for a two-terminal multi-junction "step-cell" using detailed balance method

Cite as: J. Appl. Phys. **119**, 073104 (2016); https://doi.org/10.1063/1.4942223
Submitted: 05 December 2015 . Accepted: 05 February 2016 . Published Online: 19 February 2016

Sabina Abdul Hadi, Eugene A. Fitzgerald, and Ammar Nayfeh

View Online Export Citation CrossMark

ARTICLES YOU MAY BE INTERESTED IN

Detailed Balance Limit of Efficiency of p-n Junction Solar Cells
Journal of Applied Physics **32**, 510 (1961); https://doi.org/10.1063/1.1736034

Limiting efficiencies of ideal single and multiple energy gap terrestrial solar cells
Journal of Applied Physics **51**, 4494 (1980); https://doi.org/10.1063/1.328272

A 2-terminal perovskite/silicon multijunction solar cell enabled by a silicon tunnel junction
Applied Physics Letters **106**, 121105 (2015); https://doi.org/10.1063/1.4914179

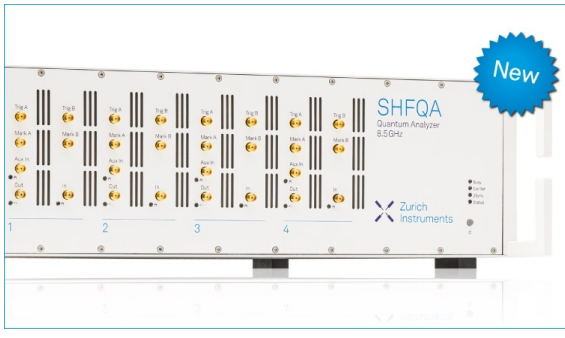

Your Qubits. Measured.
Meet the next generation of quantum analyzers
- Readout for up to 64 qubits
- Operation at up to 8.5 GHz, mixer-calibration-free
- Signal optimization with minimal latency

Find out more
Zurich Instruments

© 2016 AIP Publishing LLC.

Theoretical efficiency limit for a two-terminal multi-junction "step-cell" using detailed balance method

Sabina Abdul Hadi,[1] Eugene A. Fitzgerald,[2] and Ammar Nayfeh[1]
[1]*Institute Center for Future Energy Systems (iFES), Department of Electrical Engineering and Computer Science (EECS), Masdar Institute of Science and Technology, P.O. Box 54224, Abu Dhabi, United Arab Emirates*
[2]*MIT Microsystems Technology Laboratories, Cambridge, Massachusetts 02139, USA*

(Received 5 December 2015; accepted 5 February 2016; published online 19 February 2016)

Here we present detailed balance efficiency limit for a novel two-terminal dual and triple junction "step-cell" under AM 1.5G and AM 0 incident spectrums. The step-cell is a multi-junction (MJ) solar cell in which part of the top cell is removed, exposing some of the bottom cell area to unfiltered incident light, thus increasing bottom cell's photogenerated current. Optical generation of the bottom cell is modeled in two parts: step part, limited by the bottom cell bandgap, and conventional part, additionally limited by the top cell absorption. Our results show that conventionally designed MJ cell with optimized bandgap combination of 1.64 eV/0.96 eV for dual junction and 1.91 eV/1.37 eV/0.93 eV for triple junction has the highest theoretical efficiency limit. However, the step-cell design provides significant efficiency improvement for cells with non-optimum bandgap values. For example, for 1.41 eV (~GaAs)/Si dual junction under AM 1.5G, efficiency limit increases from ~21% in a conventional design to 38.7% for optimized step-cell. Similar benefits are observed for three-junction step-cell and for AM 0 spectrum studied here. Step-cell relaxes bandgap requirements for efficient MJ solar cells, providing an opportunity for a wider selection of materials and cost reduction. © *2016 AIP Publishing LLC*. [http://dx.doi.org/10.1063/1.4942223]

I. INTRODUCTION

Currently, multi-junction (MJ) solar cells have the highest reported experimental and theoretical efficiencies. The advantage of stacking two or more solar cells (sub-cells) on top of each other is that the lattice thermalization losses are reduced due to tuning of the sub-cell bandgaps to the energy of incident photons, $E = h\nu$ (where h is Planck's constant and ν is the frequency of incident light). When sub-cells are connected in series, we have a two terminal (2T) device, which can be utilized through monolithic growth of sub-cells or via bonding of individually fabricated cells. The efficiency of MJ solar cells connected in series is limited by the lowest current generated in one of the sub-cells. Therefore, for optimum performance of a 2T MJ solar cell, current matching in sub-cells is required. In a traditional 2T MJ cell design, where sub-cells have equal areas, current-matching condition imposes restrictions in the selection of the energy bandgap, E_g, and absorber thicknesses of sub-cells.

Various models have been used in the past to calculate the theoretical upper efficiency limit of traditional MJ solar cells connected in series.[1–6] Detailed balance method is used to determine the thermodynamic limiting efficiency of a solar cell design.[1,2] For detailed balance, it is assumed that each sub-cell absorbs all the photons with energies above its bandgap, while all the photons with energies below the bandgap are fully transmitted. It was shown in Ref. 3 that optimal properties of MJ stack can be achieved if each sub-cell's rear surface is a perfect reflector that reflects the light emitted by a sub-cell back on itself while allowing photons of energy lower than its bandgap to pass through to underlaying sub-cells. Based on detailed balance, the maximum theoretical upper efficiency limit of an ideal 2T dual-junction (2J) solar cell was estimated to be ~42%–45%, for a design with the top cell $E_g \sim 1.6$–1.64 eV and bottom cell $E_g \sim 0.94$–0.96 eV.[4–6] Optimum bandgap combination and maximum efficiency reported in the literature vary slightly depending on the model and assumptions used during calculations. Similarly, optimum bandgaps for a three-junction solar cell were calculated to be ~1.90/1.36/0.94 eV for top, middle, and bottom cells, respectively.[4,5]

Multi-junction cells are still mostly limited to niche applications in space and for concentrated solar power, due to their inherently high costs. In order to make MJ solar cells commercially available, efforts are being made to achieve high conversion efficiency (η) at a lower cost by using abundant materials such as Si. Based on their bandgap and absorption properties, the most suitable choice for MJ solar applications are III-V materials. Recently, a plethora of research has been focusing on advances in III-V on Si technology.[7–16] Lattice and thermal expansion mismatch between III-V materials and Si present practical implementation challenges, due to dislocations formed during the growth. One way to overcome this challenge is to use graded buffer layers, such as $Si_{1-x}Ge_x$ layers.[7,8] However, $Si_{1-x}Ge_x$ buffer layers have bandgap smaller than that of Si and since thick buffer layers are usually required, a large part of solar spectrum is absorbed before reaching bottom Si cell.[17–20] Optical losses in those metamorphic layers can be avoided by use of wafer bonding and layer transfer of sub-cells.

In Ref. 15, we introduced a step-cell design as an alternative way to mitigate some of the losses in metamorphic layers of tandem cell and also to improve performance of

 © 2016 AIP Publishing LLC

bonded tandem cell. In a step-cell design, the bottom sub-cell is exposed to direct sunlight in order to boost the photo-generation in the bottom cell by removing some of the top cell area.[20] Figure 1 shows schematic representation of a 2J step-cell. Total area of the device (A_{total}) is composed of area of the top cell (A_{top}) and area of the exposed part of the bottom cell (A_{step}). In step-cell design, the additional level of freedom is added, relaxing the traditional design restrictions for bandgap and thickness. By optimizing step-cell efficiency through varying of the top cell area (variable A_{total}/A_{top} ratio), one can achieve competitive efficiencies while using materials with traditionally non-optimum bandgap values. The advantage of this approach is that low cost materials can be utilized for a high performing tandem cell. However, maximum efficiency of a step-cell is limited by area factor, since increasing the A_{step} increases total device area without increase in the top cell current. Furthermore, thermalization losses in a step part of the bottom cell will increase with higher A_{step} area. Hence, there is an optimum A_{total}/A_{top} ratio, depending on sub-cells' E_g and thickness, which provides maximum step-cell efficiency. Furthermore, the optimum step-cell design will vary with incident spectrum or operating conditions. By using step-cell design, the same sub-cell materials can be used for different applications by tuning A_{total}/A_{top} ratio. For example, A_{total}/A_{top} ratio can be optimized to account for the effects of specified solar concentration or for degradation effects due to space radiation. In Ref. 21, we presented theoretical upper efficiency limit of a two terminal dual junction step cell shown in Figure 1, under AM 1.5G and AM 0 conditions.

In this work, as a continuation to analysis presented in Ref. 21, the theoretical upper efficiency limit of a two terminal triple junction (3J) step cell, shown in Figure 2 is calculated. Triple junction step-cell shown in Figure 2 has middle sub-cell area chosen to be equal to the area of the top cell, A_{top}, but this does not have to be generally the case. The design in Figure 2 is chosen for simplicity and due to the fact that top cells are usually made of expensive epitaxial materials, which have tunable thickness and bandgap that is required for current matching. For practical applications, bottom cell should be made of low cost materials. Optimum area ratio of the bottom cell (A_{total}) to top cell (A_{top}) results

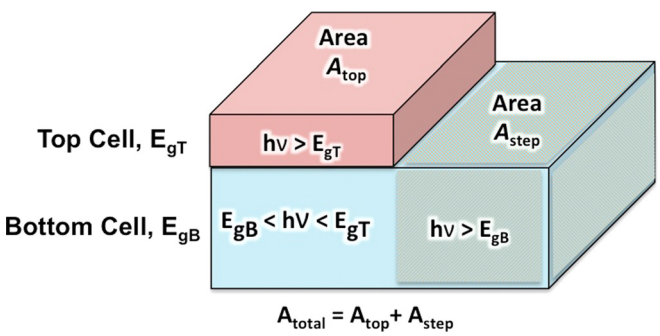

FIG. 1. Schematic representation of a two junction tandem step-cell design, showing photon energy range absorbed in each sub-cell and the step part. Top and bottom cell bandgaps are E_{gT} and E_{gB}, respectively. Top cell and bottom cell parts under the top cell have area A_{top}, while the step part of the bottom cell has area A_{step}. Total device area, $A_{total} = A_{top} + A_{step}$.

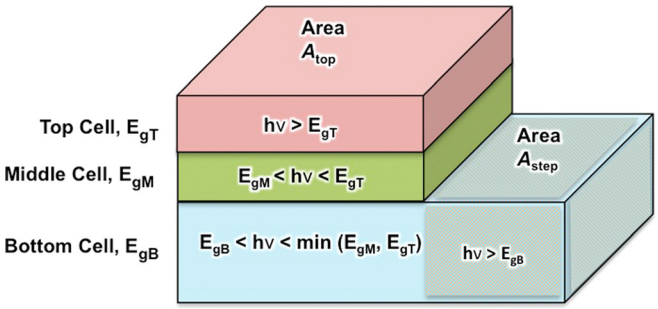

FIG. 2. Schematic representation of a tandem step-cell design for a triple junction device, showing photon energy range absorbed in each sub-cell and the step part. Top, middle, and bottom cell bandgaps are E_{gT}, E_{gM}, and E_{gB}, respectively. Top cell, middle cell, and bottom cell parts under the top cell have area A_{top}, while the step part of the bottom cell has area A_{step}. Total device area, $A_{total} = A_{top} + A_{step}$.

in sub-cell matching currents and maximum efficiency. Figure 2 also indicates respective photon energies absorbed in each of the sub-cells, in accordance with detailed balance assumptions. The top cell absorbs only photons with energies above its bandgap ($h\nu > E_{gT}$), while the middle cell responds to photons with energies between the top and middle sub-cell bandgaps ($E_{gM} < h\nu < E_{gB}$). The filtered part of the bottom cell absorbs photons unabsorbed in the top two cells but have energies that are greater than bottom cell bandgap ($E_{gB} < h\nu < \min(E_{gT}, E_{gM})$). The step part of the bottom cell absorbs all incident photons with energies larger than the bandgap of the bottom cell ($h\nu > E_{gB}$).

Theoretical study of the upper efficiency limit for ideal two terminal multi-junction step-cell presented here is based on detailed balance model, assuming that energy-pass filters are placed at the rear of each sub-cell. Energy–pass filters are perfect reflectors that reflect the thermal photons emitted by a sub-cell back onto itself while transmitting solar photons of energy lower than its bandgap to the under-laying sub-cell. Further theoretical analysis carried on here includes optimization of silicon based step-cell for AM 1.5G and AM 0 spectrum.

II. PHYSICS BASED MODELING

In order to find upper efficiency limit of our step-cell, detailed balance method is used, assuming only radiative recombination and perfect reflectors at the rear surface of each cell.[3,5] In terms of electric circuit, top, middle, and bottom cells are connected in series, as is the case in a conventional 2T MJ cell, but the bottom cell has dual optical input: one filtered by top cells and a step part having full incident spectrum. Additional electron-hole pairs (EHP) generated in a step part increase the optically generated current in the bottom cell, enhancing the limiting current of a tandem cell. Resistive losses and load effects of the sub-cells with lower current are ignored for our analysis here. Overall tandem cell current, I, is the smallest of all sub-cell currents, I_B, I_M, or I_T for bottom, middle, or top sub-cell, respectively. The voltage across the tandem cell is the sum of the open circuit voltage across all sub-cells, defined as $V = V_T + V_B$ for 2J step-cell and $V = V_B + V_M + V_T$, where V_B, V_M, and V_T are open

circuit voltages across bottom, middle, and top cell, respectively.

Detailed balance model used for calculations here includes the following assumptions, unless otherwise specified: (1) radiative recombination only; (2) all photons with energy greater than material bandgap are absorbed and those with energy lower than the material bandgap are transmitted; (3) one absorbed photon results in one electron hole pair (quantum efficiency QE = 1); (4) all emitted thermal photons are reflected back to the cell; and (5) there are no resistive and reflective losses. Incident solar spectrum standards used are AM 1.5G and AM 0 by NREL.[22]

Optically generated current in the sub-cells, I_T, I_M, and I_B, are calculated using Equations (1)–(3).[23] Bottom cell current, I_B, is generated within a step part from unfiltered incident spectrum (absorbing photons with energy $h\nu > E_{gB}$) and part under top and middle cells with filtered incident light (absorbing photons with energy $E_{gB} < h\nu < \min(E_{gM}, E_{gT})$), as shown in (3)

$$I_T = A_{top} q \int_{E_{gT}}^{\infty} F(E) QE(E) dE, \tag{1}$$

$$I_M = A_{top} q \int_{E_{gM}}^{E_{gT}} F(E) QE(E) dE, \tag{2}$$

$$I_B = A_{top} q \int_{E_{gB}}^{\min(E_{gT}, E_{gM})} F(E) QE(E) dE + A_{step} q \int_{E_{gB}}^{\infty} F(E) QE(E) dE, \tag{3}$$

where q is electron charge, E is the energy of incident photon, and F is incident spectral photon flux density, calculated from Ref. 22. Equation (3) is valid for 3J step-cell case, while for 2J device, the upper limit of the first integral is E_{gT} and rest of the expression remains the same. Short circuit current, I_{SC}, across the tandem step-cell is selected as the minimum value of the three calculated optical currents, I_B, I_M, and I_T. Current density, J, of a tandem step-cell and each sub-cell is calculated using total device area, A_{total}, and is equal to $J = I/A_{total}$.

Saturation (dark) current density of all sub-cells is calculated using the approximate expression derived from detailed balance analysis, assuming energy-pass filters at a rear sub-cell surface, shown below[3,23–25]

$$J_0 = q \frac{2\pi}{h^3 c^2} (kT)^3 \left(\frac{E_g}{kT} + 1 \right)^2 e^{-E_g/kT}, \tag{4}$$

where k is Boltzmann's constant; T = 300 K is operating temperature; E_g is bandgap of a respective sub-cell, E_{gB}, E_{gM}, or E_{gT}; and other constants have their usual meaning. Detailed steps to derive expression in (4) for dark current due to blackbody radiation are presented by King *et al.* in Ref. 25.

Current-voltage (IV) characteristics for the tandem step-cell are calculated using expression in Equation (5). Subscript i is the number of sub-cells in a tandem step-cell where I_{SCi} and I_{0i} are short circuit and saturation current of each sub-cell.[6] For 2J step-cell, I_{SCi} corresponds to I_B and I_T with i = 1–2, while for 3J case, I_{SCi} equals I_B, I_M, and I_T for i = 1–3, respectively.

$$V(I) = \frac{kT}{q} \ln \prod_{i=1}^{2,3} \left(\frac{I_{SCi} - I}{I_{0i}} + 1 \right). \tag{5}$$

The open circuit voltage, V_{oc}, of a MJ cell can be calculated by using[23]

$$V_{oc} = \frac{kT}{q} \ln \prod_{i=1}^{2,3} \left(\frac{I_{SCi}}{I_{0i}} + 1 \right). \tag{6}$$

Efficiency of the cell is found by dividing maximum output power density $P_{max} = I_{max} V_{max}/A_{total}$ by input power of given incident spectrum.

III. RESULTS AND DISCUSSION

Theoretical analysis here is done for general case of a 2J and 3J step-cell, with special emphasis on Si based tandem step-cell. Analysis was carried out for terrestrial and space conditions. Input AM 1.5G and AM 0 spectrum from NREL[22] are taken in the range between 280 and 2000 nm and are interpolated with a 5 nm equal wavelength step. Input optical power is taken to be 1000 W/m^2 for AM 1.5G and ~1349 W/m^2 for AM 0 spectrum. Variable parameters included sub-cell bandgaps, A_{total}/A_{top} ratio, and incident spectrum.

A. 2J step-cell under AM 1.5G and AM 0 spectrum

Figure 3 shows the upper efficiency limit (circles) for 2J step-cell with optimized bandgap combinations for each A_{total}/A_{top} = 1–2, under AM 1.5G incident spectrum and T = 300 K. Horizontal axis shows optimum bottom and top cell bandgaps, E_{gB} and E_{gT} for each A_{total}/A_{top} value. Figure 3 also shows the efficiency upper limit of a traditionally designed tandem cell ($A_{total} = A_{top}$, stars) for the same sub-cell bandgap combinations. Maximum efficiency of ~46% is achieved for conventional tandem cell design ($A_{total}/A_{top} = 1$) with ~0.96 eV bottom and ~1.65 eV top cell bandgaps. However, when top and bottom cell bandgaps vary from the optimized values, step-cell design provides significant advantage. As A_{total}/A_{top} ratio increases, the energy gap difference between top and bottom cell bandgaps decreases.[21] Note that when A_{total}/A_{top} ratio = 2, optimum top cell bandgap is very close to that of the bottom cell; hence, efficiency limit (~34%.) of a single junction cell is achieved with a bandgap of ~1.34 eV.

Theoretical upper efficiency limit of 2J tandem step-cell is calculated for AM 0 incident spectrum. Figure 4 compares upper efficiency limit and optimized sub-cell bandgaps of tandem step-cell under AM 1.5G and AM 0 spectrum, for each A_{total}/A_{top} ratio. Step-cell performance dependence on

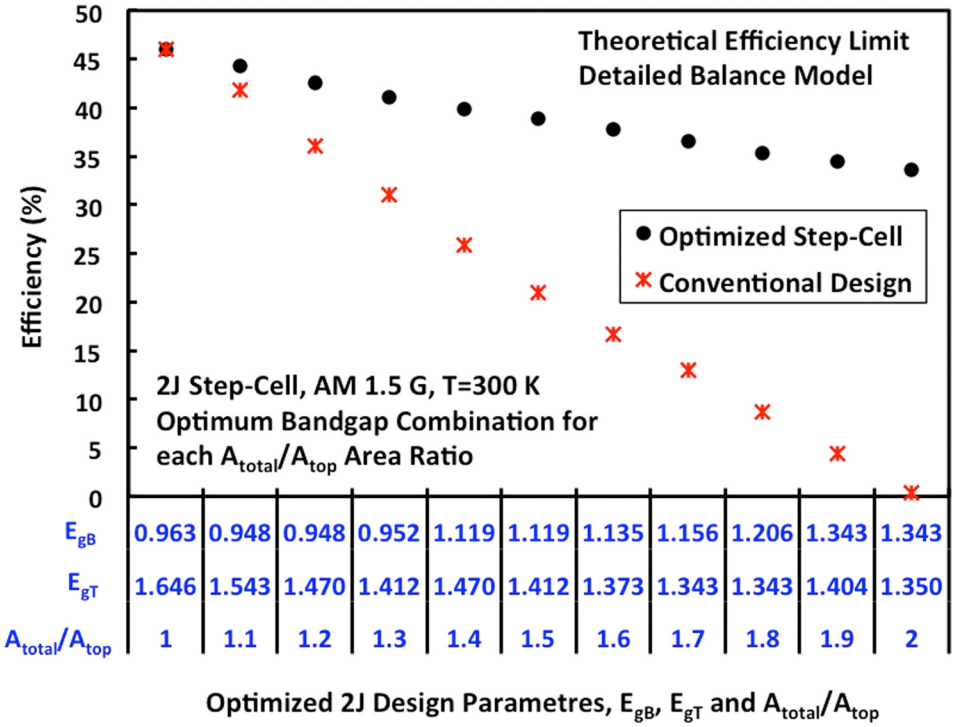

FIG. 3. Upper efficiency limit for 2J step-cell with optimized bandgap combinations for each $A_{total}/A_{top} = 1$–2 ratio, under AM 1.5G incident spectrum and $T = 300\,K$ (circles). Horizontal axis shows optimum bottom and top cell bandgaps, E_{gB} and E_{gT} for each A_{total}/A_{top} value. Also shown is the efficiency upper limit of a conventional tandem cell ($A_{total} = A_{top}$) for selected sub-cell bandgap combinations (stars).

the A_{total}/A_{top} area ratio and optimum sub-cell bandgaps are similar for both incident spectrums, with slightly lower conversion efficiency for AM 0 standard. Maximum achievable conversion efficiency under AM 0 spectrum is ~43% for $E_{gT} \sim 1.61\,eV$ and $E_{gB} \sim 0.92\,eV$ for conventional tandem cell design ($A_{total}/At_{op} = 1$). Optimized bandgap combinations for step-cell under AM 0 are close to the values found under AM 1.5G standard illumination.

Further, efficiency upper limit is calculated for silicon-based step-cell. Figure 5 shows efficiency upper limit of silicon based 2J step-cell (full lines) for optimum A_{total}/A_{top} ratios (dotted lines) as a function of top cell bandgap, for AM 1.5G and AM 0 incident spectrum (black and red lines, respectively) at $T = 300\,K$. For comparison, the efficiency of traditionally designed Si-based tandem cell ($A_{total} = A_{top}$) for both incident spectrums is shown (dashed lines). Maximum efficiency limit of ~45% is achieved for traditional tandem cell and top cell bandgap $E_{gT} \sim 1.74\,eV$ under AM 1.5G standard. Slightly lower efficiency limit (~42%) is observed under AM 0 standard and with $E_{gT} \sim 1.77\,eV$. In Ref. 21, we compared upper efficiency limit of Si-based 2J cell with step-cell and conventional design at temperatures ranging between $T = 100$ and $400\,K$ under AM 0 standard, showing that optimum design of the Si-based step-cell cell does not vary significantly with the operating temperature. Once maximum efficiency is achieved (at $E_{gT} \sim 1.74\,eV/1.77\,eV$),

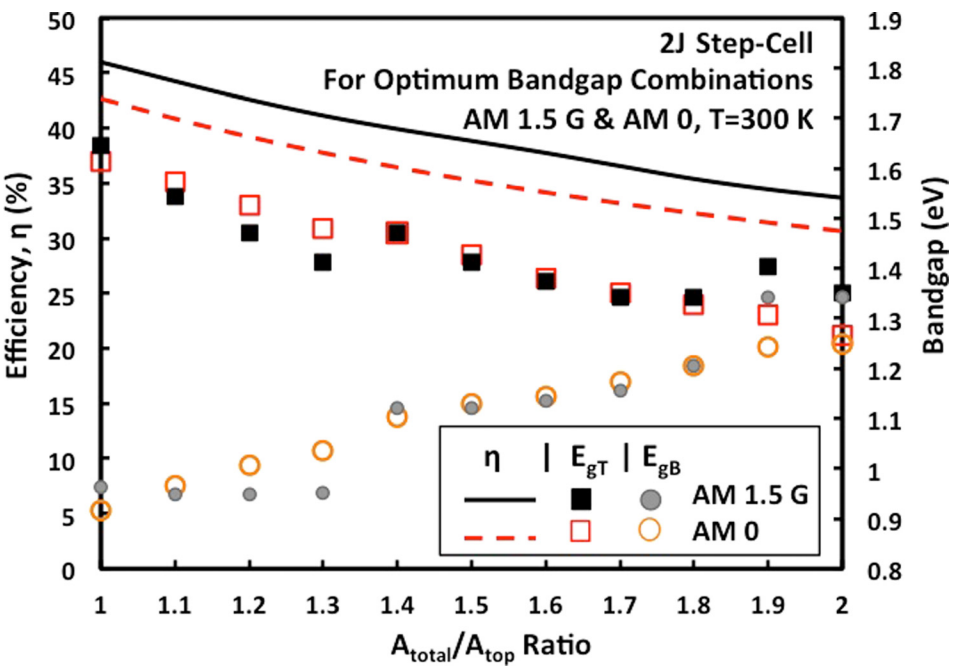

FIG. 4. Upper efficiency limit for 2J step-cell and corresponding optimized top cell E_{gT} (square) and bottom cell E_{gB} (circle) bandgaps for each A_{total}/A_{top} ratio for AM 1.5G (full) and AM 0 (dashed) input spectrum.

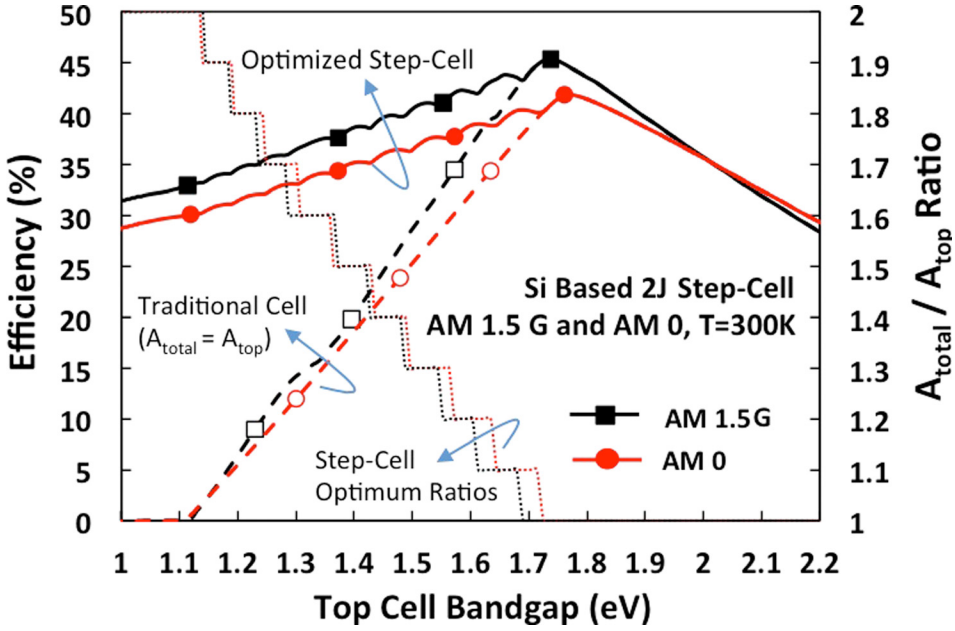

FIG. 5. Theoretical efficiency upper limit of a Si-based 2J step-cell (full lines) for optimum A_{total}/A_{top} ratio (dotted lines) as a function of a top cell bandgap, for AM 1.5G and AM 0 incident spectrum (black and red lines, respectively). Also shown is traditionally designed 2J cell (dashed lines).

conventional tandem cell becomes optimum design. This is due to the fact that optimum A_{total}/A_{top} ratio is inversely proportional to the top cell bandgap. When the E_{gT} is large, the top cell is limiting the current flow, so there is no need for bottom cell enhancement. Si-based step-cell conversion efficiency between 40% and 45% could also be achieved by non-optimized top cell bandgap ranging between 1.49 and 1.88 eV and A_{total}/A_{top} ratio ranging between 1 and 1.3. As top cell bandgap decreases, optimum A_{total}/A_{top} ratio increases indicating that less of the top cell area is needed due to larger light absorption in the top cell. Moreover, these results show flexibility and possible cost reduction in terms of the top cell material without significant loss in conversion efficiency due to step-cell design.

Step-cell design provides significant improvement for cells with non-optimized top cell bandgap values. For example, when top cell $E_{gT} = 1.41$ eV (close to the E_g of GaAs), efficiency upper limit under AM 1.5G spectrum increases from ~21% in conventional design ($A_{total}/A_{top} = 1$) to ~38.7% for a step-cell with $A_{total}/A_{top} = 1.5$ (Figure 6).

B. 3J Step-cell under AM 1.5G and AM 0 spectrum

Theoretical efficiency upper limit for 3J two terminal step-cell, designed as in Figure 2, is analyzed under AM 1.5G and AM 0 spectrum. The results show a similar effect of area ratio as in the 2J case[21] and are displayed in Figure 7. Maximum efficiency of ~52% under AM 1.5G standard is achieved for $A_{total}/A_{top} = 1$ (conventional tandem cell design) with E_{gT}, E_{gM}, and E_{gB} equal to 1.91 eV, 1.37 eV, and 0.93 eV, respectively (Figure 7(a)), which is in agreement with what others have found for conventional 3J tandem cell.[4,5] For AM 0 incident spectrum, the maximum efficiency is slightly lower (~49%) and is achieved for $E_{gT} \sim 1.84$ eV, $E_{gM} \sim 1.20$ eV, and $E_{gB} \sim 0.75$ eV with conventional tandem design (Figure 7(b)).

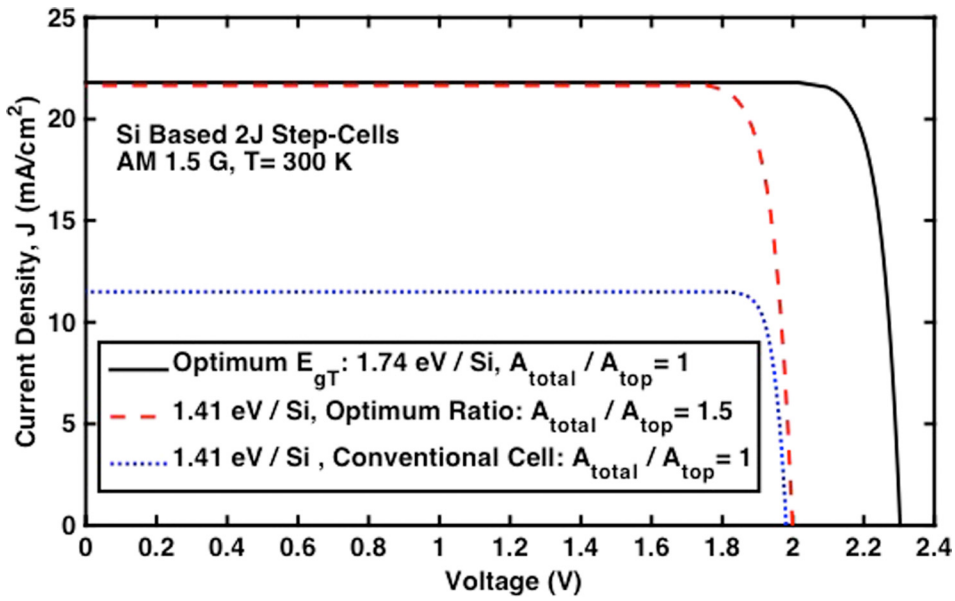

FIG. 6. Current density–voltage characteristics of a Si-based 2J step-cell for AM 1.5G standard, with optimum top cell bandgap, $E_{gT} = 1.74$ eV (full line), and non-optimum top cell bandgap, $E_{gT} = 1.41$ eV for optimum A_{total}/A_{top} ratio = 1.5 (dashed line) and A_{total}/A_{top} ratio = 1 (dotted line).

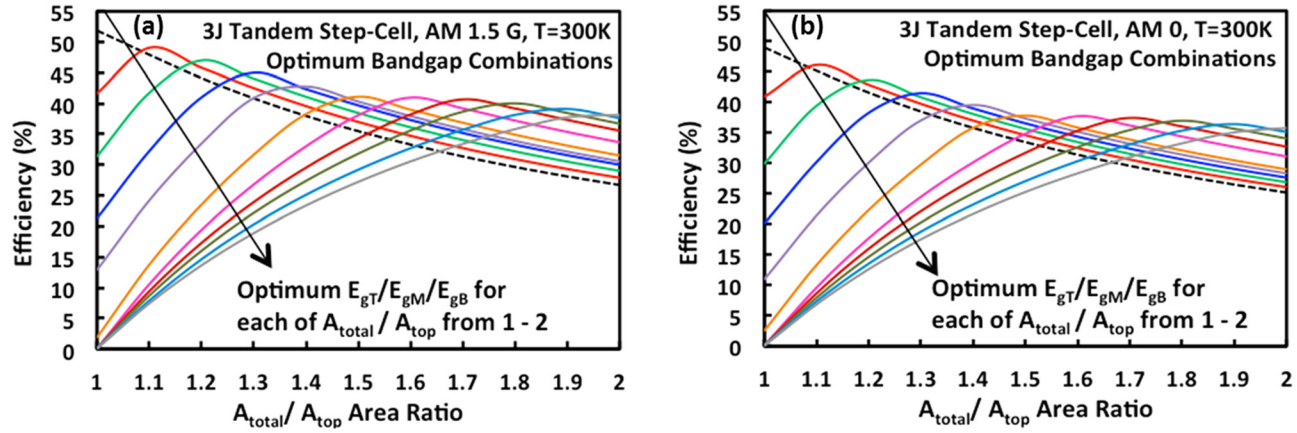

FIG. 7. Efficiency upper limit of a 3J step-cell as a function of A_{total}/A_{top} ratio for optimized bandgap combinations for each A_{total}/A_{top} ratio (from 1 to 2) for AM 1.5 G (a) and AM 0 (b) incident spectrum, at T = 300 K. Dashed line shows efficiency for a cell with $E_{gT}/E_{gM}/E_{gB}$ optimized for conventional tandem cell ($A_{total}/A_{top} = 1$).

Exposure of bottom cell provides significant improvement in the tandem cell efficiency when bandgaps of subcells are not optimized for conventional design (Figure 7, full lines). For example, step cell with $E_{gT}/E_{gM}/E_{gB}$ combination of 1.74 eV/1.12 eV/0.94 eV and area ratio $A_{total}/A_{top} = 1.3$ has efficiency of ~45% under AM 1.5G spectrum, while in conventional design ($A_{total}/A_{top} = 1$) its efficiency is ~21% (refer to Fig. 7(a), blue, 4th curve from the top).

Figure 8 shows maximum efficiency (η) of optimized step-cell and corresponding optimum bandgaps for each area ratio. Since top and middle cells are designed in conventional way, their bandgaps decrease consistently with increasing bottom cell exposure, while bottom cell bandgap increases. For area ratios > 1.5, middle cell bandgap is smaller than the bottom cell bandgap, but due to exposure of the bottom cell to unfiltered light, optical generation in bottom cell is still achieved. This confirms that step cell design is especially useful for use of graded buffer layers with low bandgap values, which can be utilized by embedding them with the middle junction.

The 3J step-cell was further studied assuming that the bottom cell is made from inexpensive Si material. Figure 9 shows theoretical efficiency of 3J Si-based traditionally designed tandem cell with $A_{total} = A_{top}$ as a function of middle and top cell bandgaps, E_{gM} and E_{gT} under AM 1.5G (a) and AM 0 (b) standard illumination. For AM 1.5G incident spectrum, the highest efficiency of a conventional tandem cell is ~50% with $E_{gM} \sim 1.5$ eV and $E_{gT} \sim 2$ eV, while for AM 0 standard maximum efficiency is slightly lower (~46%) with $E_{gM} \sim 1.5$ eV and $E_{gT} \sim 2.1$ eV. Efficiencies of conventional 3J cell with $E_{gT} < E_{gM}$ or $(E_{gM}, E_{gT}) < E_{gB\text{-}Si}$ are zero (blue regions in Figure 9).

By using step-cell design ($A_{total}/A_{top} > 1$), current in the bottom cell increases and the bandgap limitations are relaxed. Figure 10 illustrates the benefits of a step-cell where theoretical efficiency limit of Si-based 3J step-cell is shown as a function of E_{gM} and E_{gT} under AM 1.5G for different $A_{total}/A_{top} = 1.2$ (a), 1.4 (b), 1.6 (c), and 1.8 (d). As A_{total}/A_{top} ratio increases, we can observe increase in the efficiency limit of the cells with $E_{gM} < E_{gB}$ from zero in conventional design (Fig. 9(a)) to ~35%–40%, depending on the area ratio and E_{gT}/E_{gM} bandgap combination.

Figure 11 shows maximum efficiency with optimized top and middle bandgaps for each ratio for Si based 3J step-

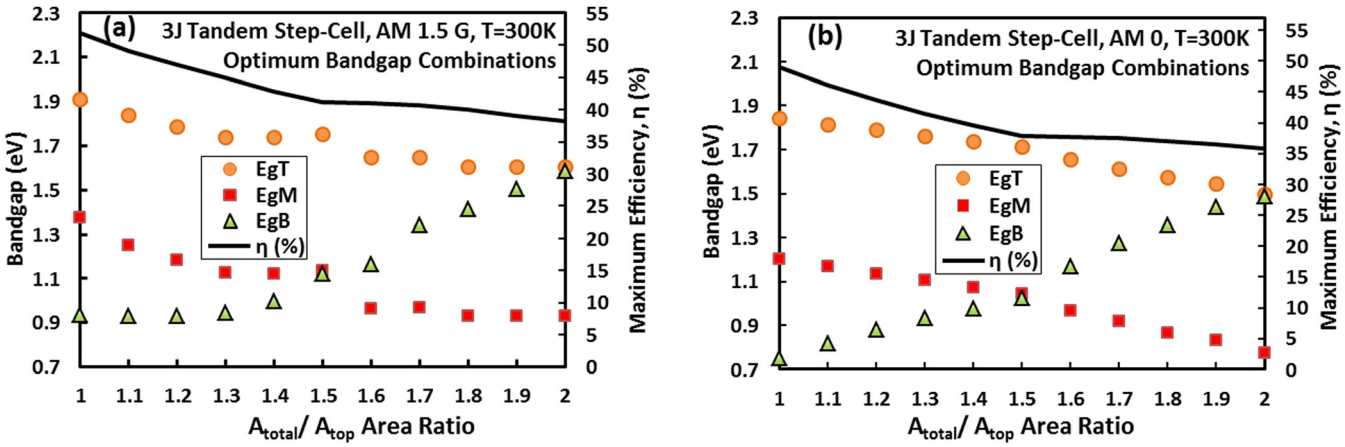

FIG. 8. Maximum efficiency limit of optimized 3J step-cell and corresponding optimum top cell (E_{gT}), middle cell (E_{gM}) and bottom cell (E_{gB}) bandgaps for each A_{total}/A_{top} ratio under AM 1.5G (a) and AM 0 (b) incident spectrum, at T = 300 K.

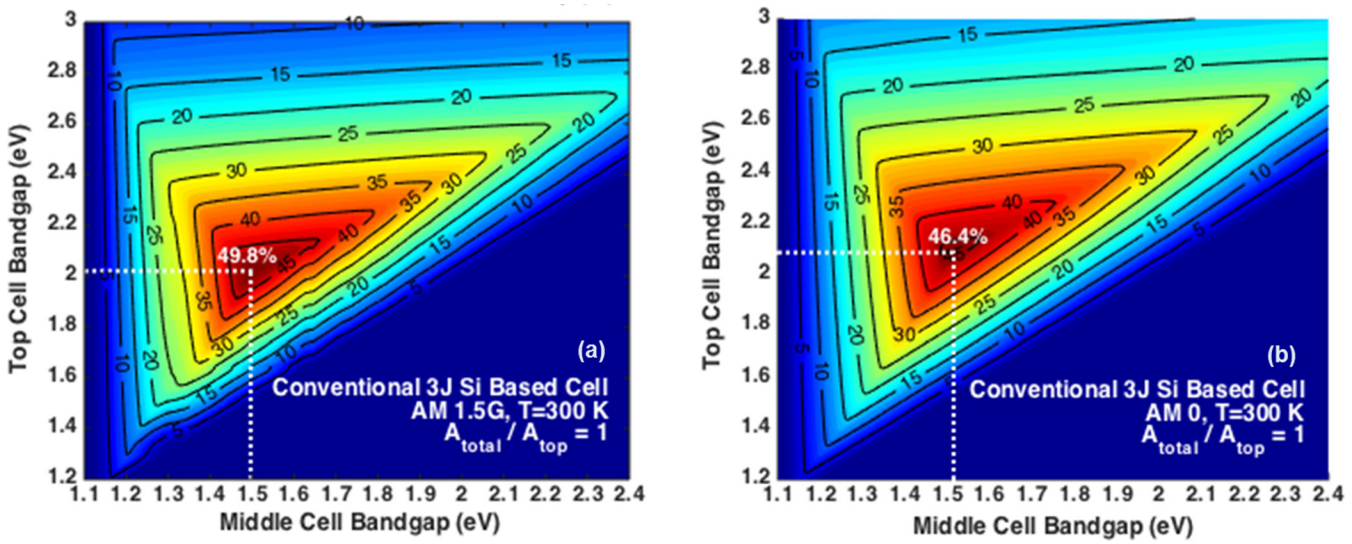

FIG. 9. Theoretical efficiencies of 3J Si-based traditionally designed tandem cell with $A_{total} = A_{top}$ as a function of middle and top cell bandgaps, E_{gM} and E_{gT} under AM 1.5G (a) and AM 0 (b) incident spectrum.

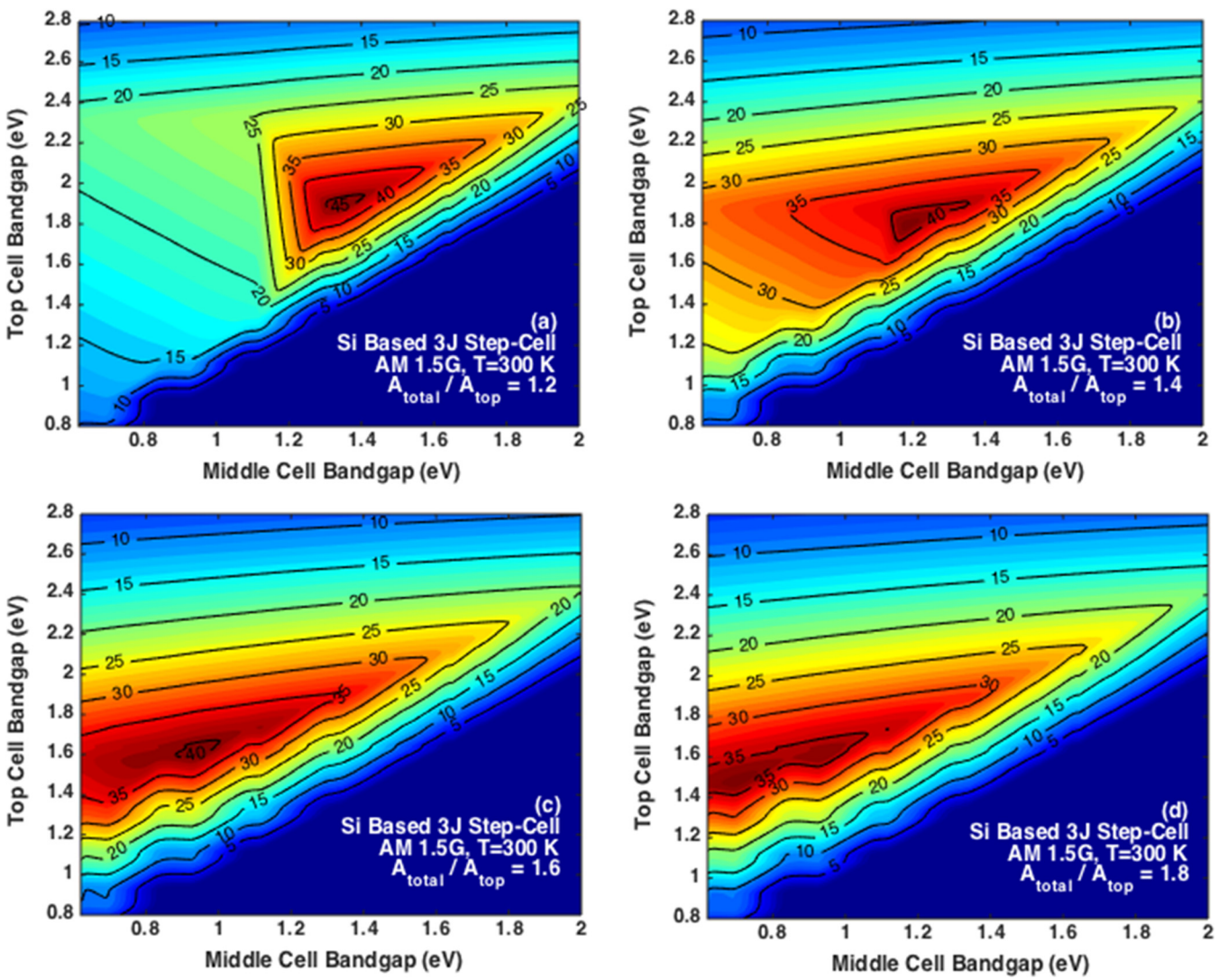

FIG. 10. Theoretical efficiencies of 3J Si-based tandem step-cell as a function of middle and top cell bandgaps, E_{gM} and E_{gT} under AM 1.5 G for different $A_{total}/A_{top} = 1.2$ (a), 1.4 (b), 1.6 (c), and 1.8 (d).

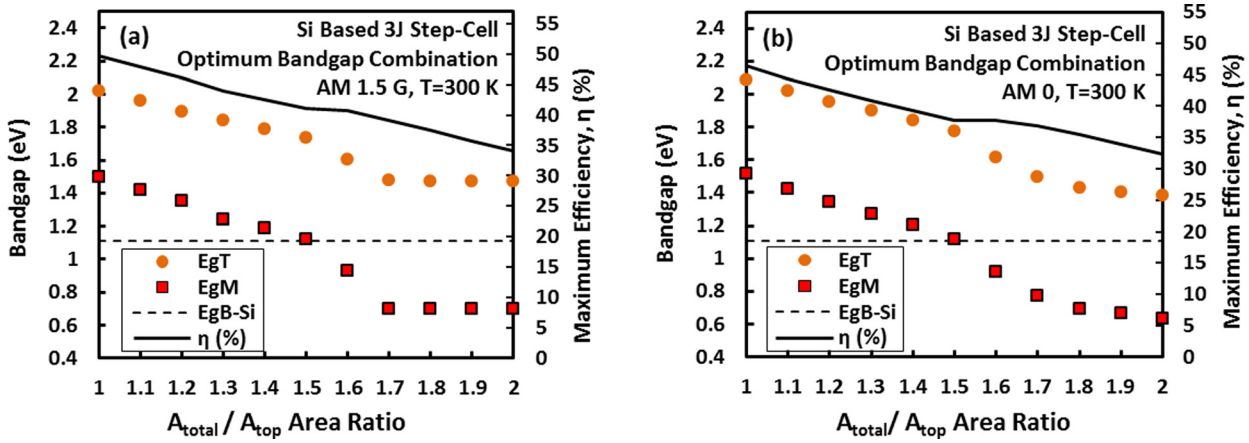

FIG. 11. Maximum efficiency limit of optimized 3J Si based step-cell and corresponding top cell (E_{gT}), middle cell (E_{gM}) and bottom Si cell ($E_{gB\text{-}Si}$) bandgaps for each A_{total}/A_{top} ratio for AM 1.5G (a) and AM 0 (b) incident spectrum.

cell under AM 1.5G (a) and AM 0 (b) spectrum. Figure 11 illustrates that even MJ cells with middle bandgap lower than the bottom Si cell bandgap (as is the case when SiGe buffer layers are used for III-V growth on Si) can theoretically provide efficiencies up to 40% if the step-cell design is used and area ratio, A_{total}/Atop, is larger than 1.5. For $A_{total}/A_{top} > 1.7$, optimum sub-cell bandgap combination does not change, indicating that beyond this area ratio, step-cell's performance cannot be further optimized because of fixed bottom cell bandgap, so overall efficiency decreases due to total area factor. While trends for both bandgap and efficiency are similar in Figures 11(a) and 11(b), there are slight variations in optimum bandgap and maximum efficiency due to different incident spectra.

IV. CONCLUSION

In conclusion, theoretical analysis for upper efficiency limit of a novel 2 terminal dual and triple junction step-cell under AM 1.5G and AM 0 illumination standard is calculated using physics based detailed balance method. Conventional tandem cell with optimized bandgap combination has the highest theoretical efficiency. Under AM 1.5G incident spectrum, the highest efficiency is ~46% for 2J cell with 1.64/0.96 eV bandgap combination and ~52% for 3J cell with 1.91/1.37/0.93 eV combinations. However, our results show that step-cell design relaxes bandgap requirements for efficient tandem cell and allows use of low bandgap material as a middle cell, which is especially useful for monolithic MJ solar cells with metamorphic buffer layers. Optimized step-cell design can provide close to ideal upper efficiency limits for cells with non-optimized top-cell E_g values. For example, for 2J Si-based step-cell with top cell $E_{gT} = 1.41$ eV (~GaAs) under AM 1.5G illumination, efficiency upper limit increases from ~21% in conventional design ($A_{total}/A_{top} = 1$) to 38.7% for a step-cell with $A_{total}/A_{top} = 1.5$. Similarly, 3J cell with conventionally non-optimized $E_{gT}/E_{gM}/E_{gB}$ bandgap combination of 1.74 eV/1.12 eV/0.94 eV has efficiency limit increased from ~21% for $A_{total}/A_{top} = 1$ (traditional design) to ~45% for $A_{total}/A_{top} = 1.3$ (step-cell design) under AM 1.5G incident spectrum. Furthermore, analysis of 2J and 3J step-cells under AM 0 spectrum showed that the optimum bandgap combination does not change significantly and step-cell design provides similar benefits compared to analysis under AM 1.5G standard. Finally, step-cell design provides opportunity for wider selection of materials used in tandem solar cell applications, with potential for added cost benefits and increased flexibility in design requirements.

[1]W. Shockely and H. J. Queisser, "Detailed balance limit of efficiency of p-n junction solar cells," J. Appl. Phys. **32**, 510 (1961).
[2]C. H. Henry, "Limiting efficiencies of ideal single and multiple energy gap terrestrial solar cells," J. Appl. Phys. **51**, 4494 (1980).
[3]A. Marti and G. L. Araujo, "Limiting efficiencies for photovoltaic energy conversion in multigap systems," Sol. Energy Mater. Sol. Cells **43**, 203–222 (1996).
[4]C. Feser, J. Lacombe, K. Maydell, and C. Agert, "A simulation study towards a new concept for realization of thin film triple junction solar cells based on group IV elements," Prog. Photovoltaics **20**, 74–81 (2012).
[5]A. S. Brown and M. A. Green, "Detailed balance limit for the series constrained two terminal tandem solar cell," Phys. E **14**(1–2), 96–100 (2002).
[6]J. P. Connolly, D. Mencaraglia, C. Renard, and D. Bouchier, "Designing III–V multijunction solar cells on silicon," Prog. Photovoltaics **22**, 810–820 (2014).
[7]J. A. Carlin *et al.*, "High efficiency GaAs-on-Si solar cells with high V_{oc} using graded GeSi Buffers," in *28th IEEE Photovoltaic Specialists Conference* (IEEE, 2000), pp. 1006–1011.
[8]C. L. Andre, D. M. Wilt, A. J. Pitera, M. L. Lee, E. A. Fitzgerald, and S. A. Ringel, "Impact of dislocation densities on n^+/p and p^+/n junction GaAs diodes and solar cells on SiGe virtual substrates," J. Appl. Phys. **98**(1), 014502 (2005).
[9]T. J. Grassman *et al.*, "Progress toward a Si-Plus architecture: Epitaxially-integrable Si sub-cells for III-V/Si multijunction photovoltaics," in 40th IEEE Photovoltaic Specialists Conference, 2014.
[10]J. F. Geisz, J. M. Olson, M. J. Romero, C. S. Jiang, and A. G. Norman, "Lattice-mismatched GaAsP solar cells grown on silicon by OMVPE," in *4th IEEE World Conference on Photovoltaic Energy Conversion,* 2006, pp. 772–775.
[11]T. J. Grassman, J. A. Carlin, C. Ratcliff, D. J. Chmielewski, and S. A. Ringel, "Epitaxially-grown metamorphic GaAsP/Si dual-junction solar cells," in *IEEE 39th Photovoltaic Specialists Conference (PVSC), Tampa, FL, 2013*, pp. 0149–0153.
[12]D. Cheong, J. Rideout, S. Tavakoli, R. Kleima, and J. Yang, "Silicon-based multi-junction solar cell with 19.7% efficiency at 1-Sun using areal current matching for 2-terminal operation," in *2011 IEEE Photovoltaic Specialists Conference* (IEEE, 2011), pp. 001019–001024.
[13]M. Diaz *et al.*, "Dual-junction GaAsP/SiGe on silicon tandem solar cells," in *40th IEEE Photovoltaic Specialists Conference, Denver, 2014*, pp. 0827–0830.
[14]S. Abdul Hadi, T. Milakovich, M. T. Bulsara, S. Saylan, M. S. Dahlem, E. A. Fitzgerald, and A. Nayfeh, "Design optimization of single-layer

antireflective coating for $GaAs_{1-x}P_x$/Si tandem cells with x = 0, 0.17, 0.29, and 0.37," IEEE J. Photovoltaics **5**(1), 425–431 (2015).
[15]S. Abdul Hadi, E. Polyzoeva, T. Milakovich, M. Bulsara, J. L. Hoyt, E. A. Fitzgerald, and A. Nayfeh, "Novel $GaAs_{0.71}P_{0.29}$/Si tandem step-cell design," in *40th IEEE Photovoltaic Specialists Conference, 2014*, pp. 1127–1131.
[16]S. Saylan, T. Milakovich, S. Abdul Hadi, A. Nayfeh, E. A. Fitzgerald, and M. S. Dahlem, "Multilayer antireflection coating design for $GaAs_{0.69}P_{0.31}$/Si dual-junction solar cells," Sol. Energy **122**, 76–86 (2015).
[17]S. Abdul Hadi, P. Hashemi, N. DiLello, A. Nayfeh, and J. L. Hoyt, "Effect of c-$Si_{1-x}Ge_x$ thickness grown by LPCVD on the performance of thin-film a-Si/c-$Si_{1-x}Ge_x$/c-Si heterojunction solar cells," MRS Proc. **1447** (2012); available at http://journals.cambridge.org/action/displayAbstract?fromPage=online&aid=8609083&fulltextType=RA&fileId=S1946427412011633.
[18]S. Abdul Hadi, P. Hashemi, N. DiLello, A. Nayfeh, and J. L. Hoyt, "Thin film a-Si/c-$Si_{1-x}Ge_x$/c-Si heterojunction solar cells with Ge content up to 56%," *38th IEEE Photovoltaic Specialists Conference, 2012*, pp. 5–8.
[19]S. Abdul Hadi, P. Hashemi, N. DiLello, E. Polyzoeva, A. Nayfeh, and J. L. Hoyt, "Thin-film $Si_{1-x}Ge_x$ HIT solar cells," Sol. Energy **103**, 154–159 (2014).
[20]E. Polyzoeva, S. Abdul Hadi, A. Nayfeh, and J. L. Hoyt, "Reducing optical and resistive losses in graded silicon-germanium buffer layers for silicon based tandem cells using step-cell design," AIP Adv. **5**, 057161 (2015).
[21]S. Abdul Hadi, T. Milakovich, M. Bulsara, E. Polyzoeva, E. A. Fitzgerald, J. L. Hoyt, and A. Nayfeh, "Theoretical efficiency limits of a 2 terminal dual junction step cell," in 42nd IEEE Photovoltaic Specialists Conference, 2015.
[22]See http://rredc.nrel.gov/solar/spectra/ for Reference Solar Spectra: Air Masss Zero (ASTM E490) and Air Mass 1.5 (ASTM G-173-03).
[23]J. Nelson, *The Physics of Solar Cells*, 1st ed. (Imperial College Press, London, UK, 2003).
[24]S. Kurtz, D. Myers, W. E. McMahon, J. Geisz, and M. Steiner, "A comparison of theoretical efficiencies of multi-junction concentrator solar cells," Prog. Photovoltaics **16**, 537–546 (2008).
[25]R. R. King, D. Bhusari, A. Boca, D. Larrabee, X. Q. Liu, W. Hong, C. M. Fetzer, D. C. Law, and N. H. Karam, "Band gap-voltage offset and energy production in next-generation multijunction solar cells," Prog. Photovoltaics **19**, 797–812 (2011).